Superconducting dome and pseudogap endpoint in Bi2201

M. Berben,[1,*] S. Smit,[2,*] C. Duffy,[1] Y.-T. Hsu,[1] L. Bawden,[2] F. Heringa,[2] F. Gerritsen,[2] S. Cassanelli,[2] X. Feng,[2] S. Bron,[2] E. van Heumen,[2] Y. Huang,[2] F. Bertran,[3] T. K. Kim,[4] C. Cacho,[4] A. Carrington,[5] M. S. Golden,[2] and N. E. Hussey[1,5,†]

[1]*High Field Magnet Laboratory (HFML-EMFL) and Institute for Molecules and Materials, Radboud University, Toernooiveld 7, 6525 ED Nijmegen, Netherlands*

[2]*Van der Waals–Zeeman Institute, Institute of Physics, University of Amsterdam, Postbus 94485, 1090 GL Amsterdam, Netherlands*

[3]*Synchrotron-SOLEIL, L'Orme des Merisiers, Saint-Aubin 91192, France*

[4]*Diamond Light Source, Harwell Campus, Didcot OX11 0DE, United Kingdom*

[5]*H. H. Wills Physics Laboratory, University of Bristol, Tyndall Avenue, Bristol BS8 1TL, United Kingdom*

(Received 9 September 2021; accepted 17 March 2022; published 20 April 2022)

Once doped away from their parent Mott insulating state, the hole-doped cuprates enter into many varied and exotic phases. The onset temperature of each phase is then plotted versus p—the number of doped holes per copper atom—to form a representative phase diagram. Apart from differences in the absolute temperature scales among the various families, the resultant phase diagrams are strikingly similar. In particular, the p values corresponding to optimal doping ($p^{\rm opt} \sim 0.16$) and to the end of the pseudogap phase ($p^* \sim 0.19$–0.20) are essentially the same for all cuprate families bar one: the single-layer Bi-based cuprate $Bi_{2+z-y}Pb_ySr_{2-x-z}La_xCuO_{6+\delta}$ (Bi2201). This anomaly arises partly due to the complex stoichiometry of this material and also to the different p values inferred from disparate (e.g., bulk or surface) measurements performed on samples with comparable superconducting transition temperatures T_c. Here, by combining measurements of the in-plane resistivity in zero and high magnetic fields with angle-resolved photoemission spectroscopy studies in the superconducting and normal state, we argue that the phase diagram of Bi2201 may in fact be similar to that realized in other families. This study therefore brings Bi2201 into the fold and supports the notion of universality of $p^{\rm opt}$ and p^* in all hole-doped cuprates.

DOI: 10.1103/PhysRevMaterials.6.044804

I. INTRODUCTION

The phase diagram of hole-doped cuprates is extremely rich, incorporating a host of novel states, notably the Mott insulator, d-wave superconductivity, the normal-state pseudogap, the strange metal, charge order, and stripes [1]. Out of this seeming complexity, however, a number of commonalities have emerged, particularly in relation to the actual doping levels at which certain regimes begin, end, or persist to high temperature. Chief among these (for hole-doped cuprates) are $p_1^{\rm sc}$ and $p_2^{\rm sc}$ that define the extent of the superconducting (SC) dome, $p^{\rm opt}$ where T_c reaches its maximum value of $T_c^{\rm max}$, p^*—the doping level at which the normal-state pseudogap closes—and the $1/8$ anomaly at which charge/stripe order is most robust. Remarkably, despite the marked differences in crystal chemistry, structural inhomogeneity, electrical anisotropy, and fermiology, these values exhibit very little variation across multiple cuprate families. For the majority of hole-doped cuprates, the superconducting dome is believed to follow a universal parabolic curve with $p_1^{\rm sc} = 0.05$, $p^{\rm opt} = 0.16$, and $p_2^{\rm sc} = 0.27$ for both single-layer and bilayer cuprates [2]. This so-called Presland formula is largely based on the $T_c(x)$ relation found in $La_{2-x}Sr_xCuO_4$ (LSCO) for which the relation between x and p is believed to be exact in the absence of oxygen off-stoichiometry. Although deviations from this formula are observed, such as the downward dip in T_c around $p = 1/8$ [3–5], a small displacement of the dome in $Bi_2Sr_2CaCu_2O_8$ (Bi2212) [6], and an extended range of superconductivity to $p_2^{\rm sc} \sim 0.31$ in $Tl_2Ba_2CuO_{6+\delta}$ (Tl2201) [7], its application has become commonplace. Moreover, following a longstanding debate, it is now broadly accepted that, for LSCO, $YBa_2Cu_3O_{7-\delta}$ (YBCO) and its derivatives, bilayer Bi2212, and possibly $HgBa_2CuO_{4+\delta}$ (Hg1201), $p^* = 0.19$–0.20 (see Ref. [8] for a recent synopsis). This remarkable universality among diverse families of cuprates implies that at its core, the cuprate problem condenses to understanding the physics of a single CuO_4 plaquette doped beyond the parent $3d^9$ configuration with a specific number of excess holes, thereby greatly aiding the development of a unifying theoretical model.

One potential outlier in all of this is Bi2201. Due to its relatively low T_c, wide doping range, and ease of cleaving, it is one of the most heavily studied of all cuprate families. Nevertheless, its phase diagram continues to be the subject of controversy and debate. In particular, it has proved notoriously difficult to clarify the actual doping level in Bi2201. This is due in part to the distinct p values deduced from different measurement techniques but also in part due to its complex

*These authors contributed equally to this work.
†nigel.hussey@ru.nl

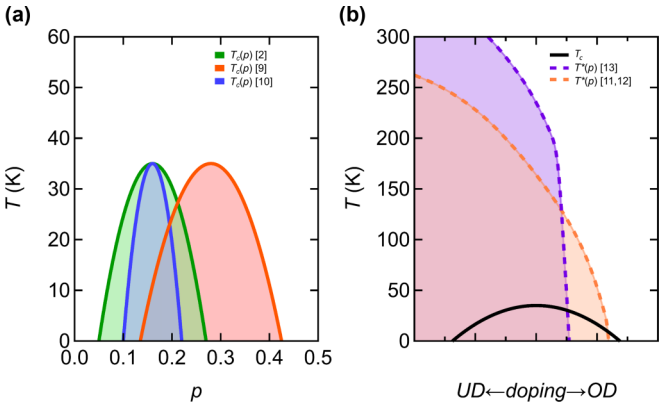

FIG. 1. Various putative phase diagrams of Bi2201. (a) Three of the proposed T_c vs p dependencies in Bi2201: (green) $T_c(p)$ as described by the Presland formula [2], (orange) $T_c(p)$ based on ARPES measurements [9], and (blue) $T_c(p)$ based on a comparison of the Hall effect in LSCO and Bi2201 [10]. (b) Two of the main proposals for the position of T^* and p^*, the end of the pseudogap phase in the (T, p) plane, based on ARPES [11] and NMR [12] (peach) and $\rho_{ab}(T)$ [13] (purple).

stoichiometry and the role of the interstitial oxygen, as well as the fact that certain constituents like bismuth can have multiple valencies. The controversy itself is summarized in Fig. 1. Panel (a) shows the three most commonly adopted proposals for the extent of the SC dome in Bi2201. The green shaded dome is based on the Presland formula with $p^{\rm opt} = 0.16$ [2]. The broad orange parabola—derived from angle-resolved photoemission spectroscopy (ARPES) measurements of the Fermi surface area [9]—suggested a SC dome in Bi2201 with p values roughly twice those found in other cuprate families, while the narrower blue-colored dome was proposed by Ando and co-workers based on comparisons of the T-dependent Hall effect in Bi2201 with those found in LSCO and Tl2201 [10]. A fourth dome, intermediate between the orange and green parabolas, has also been proposed based on scanning tunneling spectroscopy (STS) [14].

In addition to a lack of consensus on the doping dependence of T_c, the precise location of the pseudogap endpoint relative to the SC dome also remains controversial. The two most prominent proposals are illustrated in panel (b) of Fig. 1. Earlier ARPES [11] and nuclear magnetic resonance (NMR) [12,15] studies suggested that the pseudogap closes on the overdoped side for $T_c < 18$ K ($< 0.5\ T_c^{\rm max}$). Again, this would make Bi2201 something of a special case, since in most other families $p^* = 0.19$–0.20 corresponding to ∼0.85–0.90 $T_c^{\rm max}$ [8]. In-plane resistivity $\rho_{ab}(T)$ measurements, on the other hand, indicated that the S-shaped form of $\rho_{ab}(T)$—characteristic of other families inside the pseudogap phase [13,16]—vanishes in Bi2201 at a doping level corresponding to $T_c/T_c^{\rm max} \sim 0.8$, i.e., far closer to that found in other cuprates [13].

Here, we seek to provide clarity on this controversy through a combined transport and ARPES study on overdoped Bi2201 crystals in the doping range $p^{\rm opt} \leqslant p \leqslant p_2^{\rm sc}$. By comparing the magnitude and T dependence of $\rho_{ab}(T)$ with LSCO crystals with comparable T_c values, we propose a simple one-to-one correspondence between p in Bi2201 and x (the Sr content) in LSCO that agrees well with the Presland formula. Then, using high magnetic fields to differentiate between pseudogap and paraconductivity effects, we demonstrate that downturns in $\rho_{ab}(T)$ in overdoped Bi2201—previously attributed to the opening of the pseudogap—are most probably a signature of SC fluctuations. In line with the transport study, our high-resolution ARPES measurements show supporting evidence for pseudogap closure in overdoped Bi2201 in the interval $0.85 > T_c/T_c^{\rm max} > 0.65$. We also find evidence of a transformation of the antinodal energy distribution curve (EDC) line shape in the normal state above T^* similar to that reported recently in Bi2212 across p^* [17], as well as a downward jump in the magnitude of the antinodal gap below T_c.

II. EXPERIMENTAL METHODS

Large single crystals of La/Pb doped Bi2201 were grown using the floating zone technique at two different sites. The resistively-determined T_c is defined as the temperature below which the resistivity vanishes below the noise floor of our experiments. For the ARPES samples, T_c corresponds to the onset temperature of the SC transition determined by magnetic susceptibility measurements performed on the same samples (i.e., the part of the crystal cleaved off to generate a clean surface for ARPES).

Electrical contacts were made to bar-shaped samples cut from the as-grown crystals by attaching gold wires with Dupont 6838 silver paint. The contacts were then annealed in flowing O_2 at 450 °C for 10 min. All contact resistances were around 1 Ω. Typical sample dimensions were 1000 μm × 250 μm with thicknesses varying between 6 and 25 μm. A standard four-point ac lock-in detection method was used to measure the in-plane resistivity of all samples. Low field measurements were done in a 9 T CFMS system from Cryogenics. Measurements in magnetic fields up to 35 T were performed at the High Field Magnet Laboratory (HFML) at Radboud University, Nijmegen. The field was oriented perpendicular to the CuO_2 planes using a rotating sample stage and aligned using a Hall bar. The samples were cooled with a ^{4}He flow cryostat. To check for possible temperature lag in the measurement, test runs were performed in zero field—cooling and heating the samples at the same rate—and a good agreement was found.

The ARPES measurements presented in the main text were carried out at three locations: the Amsterdam laboratory using the He-Iα line at 21.2 eV with a resolution of 10 meV, the CASSIOPÉE beamline using 28 eV light at the Soleil Synchrotron under Proposal No. 20190741 with a resolution of 15 meV, and the I05 beamline at the Diamond Light Source (Proposals No. SI19403 and No. SI23742) using 22 eV light with a resolution of about 10 meV. For all measurements, linearly polarized light perpendicular to the analyzer slit was used. Careful calibration of the Fermi level was done using amorphous Au samples in electrical contact with the sample. All samples were cleaved at low temperature at pressures better then 1×10^{-10} mbar. After all temperature variations, recooling was performed and no significant aging was seen for all measurements.

III. RESULTS AND DISCUSSION

A. Doping

Early on, Obertelli *et al.* reported that the room temperature thermopower in multiple cuprates falls onto a 'universal' line when plotted versus hole doping [18], the latter set by the Presland formula [2]. Noticing that Bi2201 did not obey this universal empirical relation, Ando and co-workers proposed that a comparison of the Hall coefficient $R_H(T)$ in Bi2201 with other cuprate families (normalized to their unit cell volume) would provide a more reliable estimate of p in the former [10]. At $p = p^{opt}$, $R_H(T)$ of Bi2201 was found to coincide well with that found in both optimally doped LSCO and Tl2201, suggesting that indeed $p^{opt} = 0.16$. For doping levels away from p^{opt}, Ando *et al.* compared $R_H(T)$ in Bi2201 with corresponding curves in LSCO and concluded that the SC dome in Bi2201 is narrower, with $p_1^{sc} = 0.10$ and $p_2^{sc} = 0.22$ [10]. For $p > p^{opt}$, however, only one concentration was studied (with $T_c/T_c^{max} \sim 0.8$) and compared with LSCO $x = 0.20$.

Crucially, around this doping level, the Fermi surface of LSCO undergoes a Lifshitz transition: the Fermi level crossing the van Hove singularity (vHs) located at the zone boundary. This transition creates sections of Fermi surface with both holelike and electronlike curvature that give contributions to the Hall resistivity ρ_{xy} of opposite sign [19,20]. Indeed, the emergence of this electronlike component leads to a rapid reduction in the value of $R_H(T)$ and ultimately drives R_H negative around $p = p_2^{sc}$ [21]. By contrast, the Fermi level in Bi2201 does not cross the vHs until the edge of the SC dome [22]. Hence a comparison of $R_H(T)$ in overdoped LSCO and Bi2201 inevitably leads to a lower estimate of p in the latter. Tl2201 is another single-layer hole-doped cuprate whose Fermi surface remains holelike throughout this doping range and whose doping level is precisely known from quantum oscillation experiments (at least for $0.27 \leqslant p \leqslant 0.30$) [23]. The low-$T$ Hall effect in both the Bi2201 and Tl2201 families is found to be very similar near the edge of their respective SC domes [24], suggesting that p_2^{sc} in Bi2201 is closer to 0.30 than 0.22. As doping is reduced, however, $R_H(0)$ in both Tl2201 and Bi2201 departs significantly from the expected Drude result $[= 1/(1 + p)e]$ [24], due to either the opening of the pseudogap [25] or the onset of incoherence [26]. Irrespective of its origin, this anomalous and marked change in $R_H(0)$ in both families suggests that the Hall coefficient cannot be used to provide a reliable estimate of p, only as a guide through comparison between the two families.

Another way to estimate p is to analyze the area of the Fermi surface (an approach referred to as the Luttinger count). Systems whose band structure depends on k_z are challenging in this respect, as has been shown for LSCO [27], since then the full three-dimensional Fermi surface volume is required. Data from Hg1201 [28], Tl2201 [29], and *in situ* surface-doped Bi2212 [6] yield p $(= p_L)$ values that agree well with estimates from other techniques. For YBCO [30], LSCO [27,31], Nd-LSCO [32], and the oxychloride $Ca_{2-x}Na_xCuO_2Cl_2$ (Na-CCOC) [33], the ARPES-derived Luttinger count does not match the expected doping. Some ARPES [9] and STS [14] studies suggest a large Luttinger count in Bi2201, while others see agreement between the Luttinger count and the Presland curve [34]. Finite k_z dependence has also been argued to play a role even in materials as two-dimensional as Bi2201 [35]. Figure 3D of the Supplemental Material shows a collection of Bi2201 and LSCO Luttinger count data, including data from analogous samples to those studied here, illustrating not only the scatter between published data but also the observation that the Luttinger count often exceeds the doping level from the Presland curve, even in LSCO [36]. Table I summarizes this discrepancy for three as-measured samples from our own study [36].

TABLE I. Comparison between doping inferred from Luttinger count (p_L) and their Presland value (p_P), showing that the Luttinger counts typically return a larger value. The data and tight binding models underlying these numbers are presented in Fig. 3 of the Supplemental Material [36].

Sample	p_P (± 0.01)	p_L (± 0.03)
OD3K	0.27	0.34
OD12K	0.25	0.30
UD32K	0.14	0.24

As mentioned above, at optimal doping, both $R_H(T)$ and $\rho_{ab}(T)$ in Bi2201 agree well with those found in LSCO and Tl2201, suggesting that, for Bi2201, $p^{opt} \sim 0.16$. According to ARPES, however, the inferred doping level in Bi2201 is $\approx 50\%$ larger [9] (recall that, at optimal doping, i.e., inside the pseudogap regime, the effective carrier density is closer to p than to $1 + p$ [37].) Thus the discrepancies in the estimates of p derived from Hall and ARPES measurements—summarized in Fig. 1—are arguably the most extreme in Bi2201, thus motivating the search for an alternative means of estimating p than either Hall data or Luttinger count.

It has long been established that $\rho_{ab}(T)$ of hole-doped cuprates at optimal doping is very similar (once normalized to a single CuO_2 plane) [16,38] and that, within each family, the form of $\rho_{ab}(T)$ exhibits a systematic evolution with under- or overdoping [39]. Moreover, in contrast to the Hall resistivity, $\rho_{ab}(T)$ is relatively insensitive to Fermi surface curvature or anisotropy in the mean-free path. With this in mind, we turn to consider $\rho_{ab}(T, p)$ in Bi2201 and compare its doping and temperature dependence with that found in LSCO, whose T_c^{max} $(= 37$ K) is similar to that of Bi2201 $(T_c^{max} = 35$ K) and for which p is assumed to be equal to x. Panels (a)–(c) of Fig. 2 show a set of resistivity curves for overdoped LSCO and Bi2201 single crystals spanning the doping range $0.2 \leqslant T_c/T_c^{max} \leqslant 0.8$ and combined into pairs or groups having the same [panels (b) and (c)] or approximately the same [panel (a)] T_c value. Panels (d)–(f) of Fig. 2 show the corresponding derivatives $d\rho_{ab}/dT$. It is clear from panels (b), (c), (e), and (f) that samples with the same T_c possess an identical form of $\rho_{ab}(T)$, while in Figs. 2(a)/2(d), the form of $d\rho_{ab}/dT$ in LSCO $x = 0.21$ is found to be intermediate between that of the two Bi2201 samples.

Overall, the data reveal a systematic evolution in $\rho_{ab}(T, p)$ with a low temperature T-linear component—the (extrapolated) finite intercept in $d\rho_{ab}/dT = \alpha_1(0)$—that drops monotonically with overdoping. This T-linear component—often

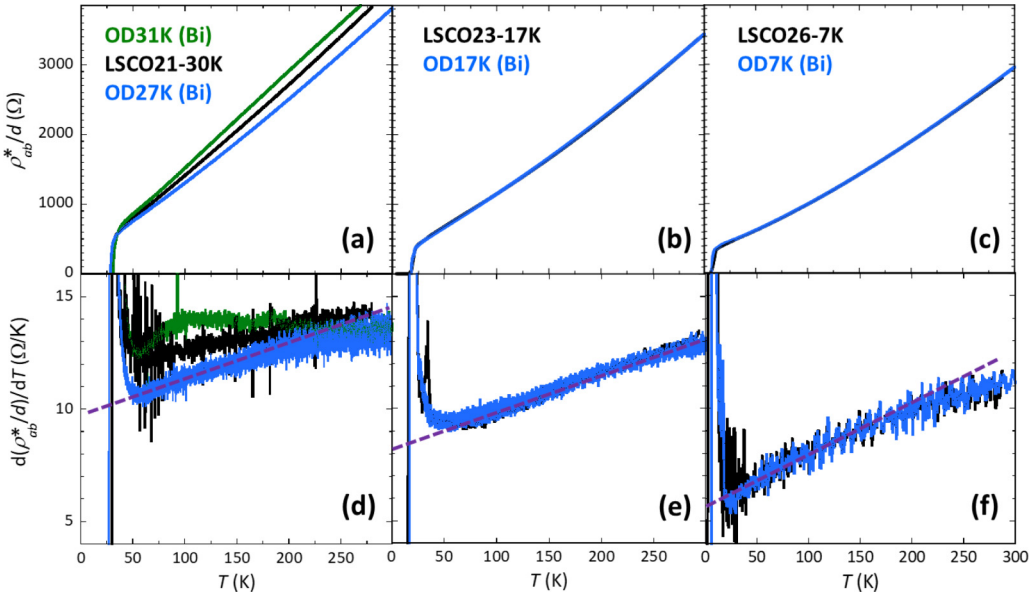

FIG. 2. Comparison of $\rho_{ab}(T, p)$ in overdoped LSCO and Bi2201. (a)–(c) $\rho_{ab}(T)$ of Bi2201 (green and blue) and LSCO (black) single crystals with similar T_c values as indicated. The x value for the LSCO samples is also included. The LSCO curves are from Refs. [40,42]. (d)–(f) Corresponding derivatives $d\rho_{ab}/dT$ for each curve. [The periodic structure in the derivative curves in panel (f) is a consequence of the thermometer calibration used in those two measurements.] The purple dashed lines imply that $\rho_{ab}(T)$ contains both T and T^2 components, with the former decreasing in magnitude with increasing doping. In all panels, each $\rho_{ab}(T)$ curve is expressed as a sheet resistance by dividing by d, the c-axis lattice parameter (=6.4 Å in LSCO and 12.3 Å in Bi2201). The asterisk on the ordinate axis of panels (a)–(c) highlights the fact that each curve has been shifted vertically to eliminate differences in residual resistivity and their slopes normalized to ensure that their derivatives coincide at room temperature. The normalization needed is typically <20%, i.e., the geometrical uncertainty, though for Bi2201-17K, it is 30%. The original Bi2201 resistivity curves are plotted in Fig. 1 of the Supplemental Material [36].

persisting to the lowest temperatures when superconductivity is suppressed by a magnetic field [40]—is one of the defining signatures of the strange metal regime of hole-doped cuprates [41]. At high-T, $d\rho_{ab}/dT$ reaches or approaches a plateau (seen most clearly in the Bi2201-31K sample) indicating a distinct regime in which $\rho_{ab}(T)$ is purely T linear, albeit with a higher slope $= \alpha_1(\infty)$. Measurements to higher temperatures ($\sim$500 K) in LSCO revealed that this high-T slope was, to within geometrical uncertainty, independent of x [42]. The ratio $\alpha_1(0)/\alpha_1(\infty)$, not prone to geometrical uncertainties, was subsequently found to decrease linearly from $\sim$1 at $p^* = 0.19$ to 0 at $p \sim 0.31$ [42].

It is clear from Fig. 2 that both this ratio and the overall form of $\rho_{ab}(T)$ in overdoped LSCO and Bi2201 are essentially identical for samples with similar T_c values across a wide doping range. The resistivity depends of course on numerous factors, not just the carrier concentration [43]. Nevertheless, given that the evolution in $\rho_{ab}(T, p)$ in hole-doped cuprates is so generic, this finding suggests strongly that LSCO and Bi2201 samples with a comparable T_c have a similar carrier density. Such reasoning is consistent with the notion that the evolution of $\rho_{ab}(T, p)$ is tied to the number of holes doped into the Mott insulator. From this, we postulate that the $T_c(p)$ dome in Bi2201 follows the Presland parabola (blue curve in Fig. 1), at least for the doping range $p^{\rm opt} \leqslant p \leqslant p_2^{\rm sc}$ and we proceed by applying the Presland formula to determine a corresponding p value (labeled hereafter as $p_{\rm P}$) from the measured T_c of each crystal [36]. This postulate, however, still leaves unresolved the discrepancy between $p_{\rm P}$ and $p_{\rm L}$. One possibility is that resistivity is governed by an effective carrier density that is different to the ARPES-derived Fermi surface, e.g., due to some of the low-lying states being incoherent (as suggested by recent high-field transport studies [24,26]). If true, one expects such a discrepancy to vanish at doping levels beyond the SC dome when all carriers are coherent. An alternative scenario, implied by the discrepancy between $p_{\rm L}$ and x in LSCO [27], is that, in certain cuprate families, the surface layers probed by ARPES have a higher carrier density than the bulk. Future studies will hopefully shed further light on this.

B. Pseudogap

Having established a $T_c(p)$ relation for overdoped Bi2201, we turn our attention to the location of the pseudogap endpoint. Key signatures of the growth of the pseudogap with decreasing doping, such as a marked drop in the specific heat jump at T_c or in the superfluid density, have yet to be reported for Bi2201. Hence here we focus on resistivity, NMR, and ARPES measurements.

By plotting the double derivative $d^2\rho_{ab}/dT^2$ as a function of hole doping, Ando and co-workers revealed that $\rho_{ab}(T)$ in underdoped Bi2201 and YBCO has a qualitatively similar S-shaped form inside the pseudogap regime with an onset temperature (and inflexion point) that decreases sharply with increasing p [13]. This S-shaped $\rho_{ab}(T)$ is a characteristic of many underdoped cuprates, including $YBa_2Cu_4O_8$ (Y124) [44], Hg1201 [16], and Bi2212 [45] and has been attributed to a reduction in the density of states and a concomitant reduction in scattering within the pseudogap regime [46]. Specifically for Bi2201, this signature of the

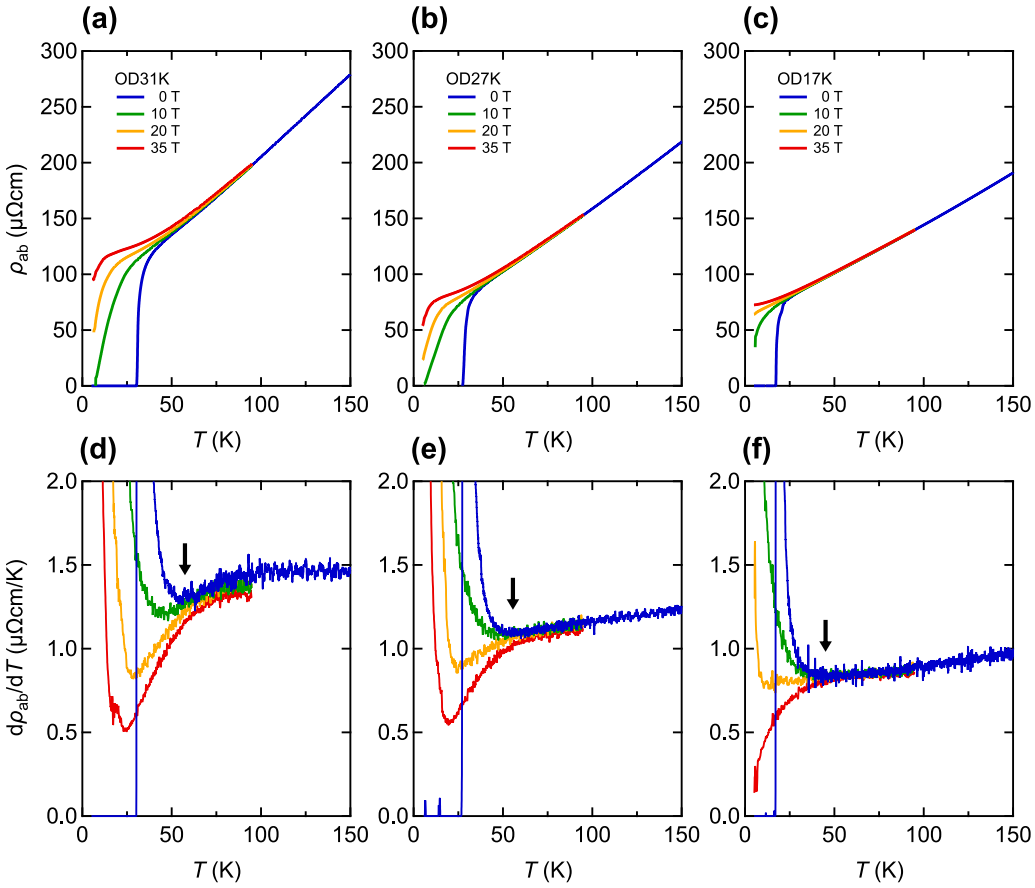

FIG. 3. Origin of the resistive downturns in Bi2201 near 60 K. (a)–(c) $\rho_{ab}(T)$ at different magnetic field strengths ($\mathbf{H}\|c$) for overdoped Bi2201 samples with T_c values of 31 K, 27 K, and 17 K, respectively [36]. (d)–(f) Corresponding derivatives $d\rho_{ab}/dT$ of the curves shown in panels (a)–(c). The black arrows indicate the approximate location of the upturns in $d\rho_{ab}/dT$ in zero field that define T_{SF}. The estimated error in T_{SF} is ±5 K. The suppression of the upturns in $d\rho_{ab}/dT$ with increasing field strength indicate that these are due to superconducting fluctuations. Note that for OD27K and OD17K, T_{SF} barely changes between 0 and 10 T. Only at field strengths of order 20 T can a clear shift in T_{SF} be seen. The downward trend in the derivative at the highest fields is due predominantly to an increasing MR as T decreases though the possibility of a small upturn in $\rho_{ab}(T)$ at the lowest temperatures cannot be excluded.

pseudogap in $\rho_{ab}(T)$ appears to vanish just beyond optimal doping [13,24,47]. The actual doping threshold for this crossover in behavior can be made more precise by inspection of Fig. 2. As evident from the derivatives plotted in Fig. 2(d), $\rho_{ab}(T)$ of OD31K ($p_P \sim 0.20$) is T linear down to around 130 K, below which $d\rho_{ab}/dT$ passes through a small but discernible maximum, corresponding to the inflexion point, around $T = 90$ K. Below $T = 60$ K, the derivative exhibits a sharper upturn due to the onset of paraconductivity contributions and the minimum in the derivative defines T_{SF}, the temperature below which SC fluctuations appear. For OD27K ($p_P \sim 0.21$), on the other hand, $d\rho_{ab}/dT$ decreases monotonically from 300 K down to $T_{SF} \sim 60$ K. This form of derivative reflects the superlinear T dependence of $\rho_{ab}(T)$ that has previously been analyzed either in terms of a single power law $1 < n < 2$ [47] or as a combination of $T + T^2$ components [24]. Importantly for the present discussion, this superlinear $\rho_{ab}(T)$ is also seen in overdoped LSCO [40] and Tl2201 [48] *outside* of the pseudogap regime. Hence the form of $\rho_{ab}(T)$ in overdoped Bi2201 changes qualitatively between $p_P = 0.20$ and 0.21 in a manner that is consistent with the closing of the pseudogap across this narrow doping window.

A decrease in the normal-state Knight shift K_s [49] or inverse spin-lattice relaxation rate $(T_1T)^{-1}$ [50] with decreasing T and p is also recognized as a prominent signature of pseudogap opening in hole-doped cuprates. NMR studies on Bi2201 [12,15,25] reported a pseudogap onset temperature T^* that decreases with increasing p, but survives deeper into the overdoped regime than inferred from the evolution of $\rho_{ab}(T, p)$. Specifically, for samples with $T_c/T_c^{max} = 0.7$ ($p_P \sim 0.22$) and 0.6 ($p_P \sim 0.23$), $T^* \sim 60$–70 K, whereas for the sample with $T_c/T_c^{max} = 0.25$ ($p_P \sim 0.255$), no drop in K_s [12] or $(T_1T)^{-1}$ [15] was observed down to the base temperature of their studies. It is noteworthy that $T^* \sim T_{SF}$ for $p_P \sim 0.22$–0.23 [36]. Moreover, for the $p_P \sim 0.23$ sample, the NMR measurements were taken in a magnetic field of 9 T [12] that is insufficient to suppress the superconductivity. This point is highlighted in Fig. 3, where a magnetic field of 10 T barely shifts T_{SF} (indicated in zero field by the black arrows and defined by the temperature below which $d\rho_{ab}/dT$ undergoes a marked upturn). SC fluctuations, like the pseudogap, cause a downturn in $\rho_{ab}(T)$ as well as a suppression of the density of states close to the Fermi level that in turn can suppress the NMR intensity [8,51]. Hence it is not possible, given the available data, to

conclude whether the drop in K_s or $(T_1T)^{-1}$ for $p_P \sim 0.23$ at $T \sim 60$ K is due to pseudogap or SC pair formation. We also note that the absolute magnitude of the drop in K_s between T_{SF} and T_c in highly overdoped Bi2201 [12] is the same as that found (and supported by spin susceptibility measurements) in highly overdoped LSCO at doping levels $x = 0.24$ and 0.26 [51] where the pseudogap has closed [36].

In order to distinguish between these two possible origins of the resistive downturns in overdoped Bi2201, we have exploited the empirical observation that, while a magnetic field suppresses superconductivity, it has little or no influence on the pseudogap itself [24,37]. Furthermore, in underdoped YBCO, for example, the magnetoresistance (MR) is found to follow a modified Kohler's rule for $T_{SF} < T < 300$ K [52] with no abrupt change across T^*. Below T_{SF}, however, the magnitude of the MR changes abruptly. Therefore, any marked change in the MR can only be due to the onset of SC fluctuations. (It should also be noted that the relative effect of paraconductivity fluctuations is much larger in materials like Bi2201 whose residual resistivities tend to be higher.) In order to resolve this ambiguity, we have measured $\rho_{ab}(T)$ on our OD31K, OD27K, and OD17K crystals in magnetic fields up to 35 T applied parallel to the c axis. Panels (a)–(c) of Fig. 3 show $\rho_{ab}(T)$ at varying field strengths with their corresponding temperature derivatives $d\rho_{ab}/dT$ shown in panels (d)–(f). For the two highest T_c samples, the upturn in $d\rho_{ab}/dT$ [downturn in $\rho_{ab}(T)$] sets in around $T \sim 60$ K (indicated by black arrows), i.e., around the same temperature as the features ascribed in the NMR studies to the opening of the pseudogap. Crucially, as H is increased, these upturns are shifted to progressively lower T. This is a strong indication that the upturns in $d\rho_{ab}/dT$ are caused by SC fluctuations with an onset temperature $T_{SF} \gtrsim 2T_c$, similar to what has been found in overdoped LSCO, for example [53]. A similar conclusion can be drawn by looking at the MR above and below T_{SF}. As shown recently [26], the normal-state MR of overdoped Bi2201 exhibits so-called H/T scaling behavior above T_{SF}, similar in form to that first reported in $BaFe_2(As_{1-x}P_x)_2$ near its putative quantum critical point [54]. As shown in Fig. 4 of the Supplemental Material [36], the MR also shows H/T scaling down to T_{SF}, below which the scaling is lost. For all measured samples, the T_{SF} values obtained by both methods are found to agree.

One notable feature of the data presented in Fig. 3 is the ubiquitous upward deviation from T linearity in $\rho_{ab}(T)$ (downturn in $d\rho_{ab}/dT$) that sets in at a temperature comparable to T_{SF}. Similar upward deviations were also observed in Bi2201 OD10K and OD18K by Lizaire *et al.*, around $T_{SF} = 25$ K and 50 K, respectively, and associated with T^*, through extrapolation of the NMR results [25]. As argued in Sec. VI of the Supplemental Material [36], where $\rho_{ab}(T)$ data for two other doping concentrations OP35K (where $T^* > T_{SF}$) and OD01K (where $T^* = 0$ K according to the NMR study [12]) are presented, these downturns in $d\rho_{ab}/dT$ appear to be a common, if not universal, feature of the low-T resistivity in Bi2201 crystals. As such, they are more likely to be a signature of localization or charge confinement (residual resistivities in Bi2201 tending to be higher than in other cuprates) rather than pseudogap formation, though the resilience of the upturns to a large magnetic field indicates that this is not a conventional form of localization [55].

Having distinguished signatures of T^* and T_{SF} in $\rho_{ab}(T, H)$, we now turn our attention to the determination of p^* from ARPES. A previous ARPES investigation of the T-dependent spectral weight for states near the zone boundary (the antinodes) concluded that, for overdoped Bi2201-22K and Bi2201-18K, spectral weight depletion sets in around 80 K and 60 K, respectively [11]. In the accompanying analysis of $\rho_{ab}(T)$, it was shown that, for Bi2201-22K, $d\rho_{ab}/dT$ departs from a T-linear dependence characteristic of overdoped (i.e., nonpseudogapped) samples around 80 K before passing through a minimum around 60 K. The authors argued that, for this sample, $T^* = 80$ K. Subsequent fluctuation analysis carried out for a sample at the same doping concentration showed that these features in the derivative could be attributed entirely to Azlamazov-Larkin SC fluctuations [24]. Hence, just as with the NMR measurements, signatures of spectral weight depletion due to pseudogap formation and due to pair formation appear to become indistinguishable in this doping range.

In order to shed further light on this issue, we have carried out a complementary ARPES study of the antinodal states in selected Bi2201 crystals. Panels (a) and (b) of Fig. 4 show, respectively, symmetrized energy distribution curves (EDCs) above and below T_c for two overdoped samples OD30K and OD23K, i.e., on either side of the resistivity-determined p^*. In the SC state, a gaplike feature is clearly visible in both samples. In OD30K, the low-energy weight remains gapped above T_c, whereas, for the more overdoped sample, this gap is effectively closed at $T \sim T_{SF} \sim 50$ K. As shown in Fig. 4(c), the gap feature in OD30K survives to $T \sim 4T_c$ and, perhaps more importantly, to $T \gtrsim 2T_{SF}$. (Recall that T_{SF} is defined here by the minimum in $d\rho_{ab}/dT$). A persistent, partial antinodal gap also emerges in Nd-LSCO ($p \sim 0.20 < p^*$) below a temperature T^* [56] that is consistent with the onset temperature for certain signatures of pseudogap physics seen in transport [57]. Similarly in Bi2201, the disappearance of the antinodal gap coincides well with the temperature ($T^* \sim 150$ K) at which $\rho_{ab}(T)$ departs from its high temperature T-linear dependence [see Fig. 2(d)]. Hence it is clear that, for $p_P \leqslant 0.20$ ($T_c \geqslant 30$ K), both ARPES and resistivity indicate the presence of an antinodal pseudogap. By contrast, for $p_P \geqslant 0.22$ ($T_c \leqslant 23$ K), signatures of a normal-state pseudogap appear to be absent in both transport and ARPES.

In closely related Bi2212, recent ARPES studies of the normal state revealed that p^* also marks a sharp, T-independent transition from incoherent antinodal spectra to more conventional metallic states [17]. In panels (e) and (f) of Fig. 4, we plot the normal-state dispersion for our two samples above the temperature at which any gap signatures are observed. Both spectra show an ungapped, parabolic dispersion, with clearly identifiable Fermi momenta in their momentum distribution curves (MDCs) at the Fermi level [Fig. 4(h)]. For OD30K, however, the EDCs are significantly broadened [Fig. 4(g)], to the point where no quasiparticle peak is identifiable and the entire spectrum is incoherent, as found for the bonding band in Bi2212 [17]. In Fig. 6 of the Supplemental Material [36], we show that this discrepancy in the EDC line shapes is not present near the nodal points on either side of p^*, where for all dopings the EDC show a conventional peaked line shape. This

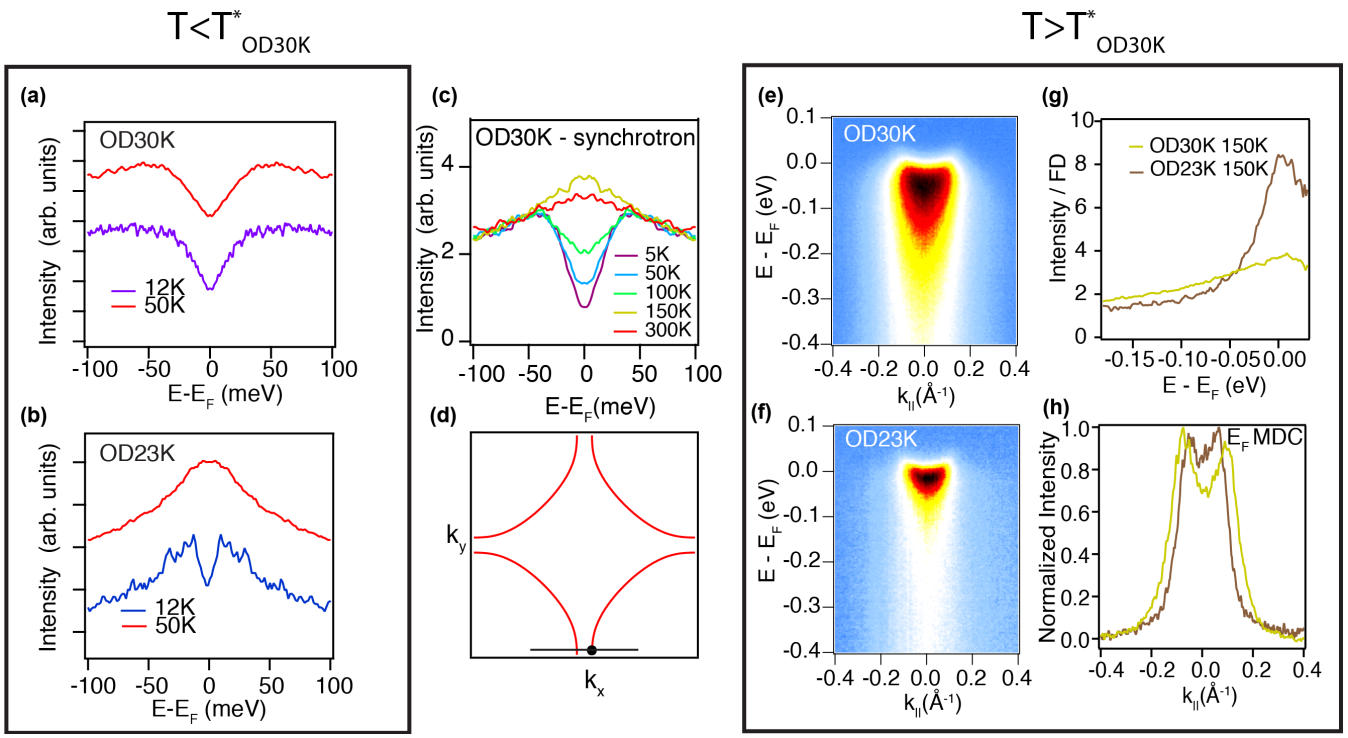

FIG. 4. Antinodal ARPES spectra across p^* in Bi2201. (a),(b) Symmetrized EDCs at the antinodal Fermi wave vector k_F [see panel (d)] for OD30K ($p_P \sim 0.20$) and OD23K ($p_P \sim 0.22$), measured both within the SC state and at $T \sim 2T_c$. (c) T-dependent symmetrized EDC at the antinode of OD30K showing the closing of the pseudogap between 100 K and 150 K. (d) Schematic of the first Brillouin zone of Bi2201, with its single band Fermi surface. The black line indicates the k-space cut measured and the black dot the locus of the EDCs. (e),(f) High-T (150 K) antinodal dispersions for OD30K and OD23K, with (g) EDCs at k_F, after division by the Fermi-Dirac distribution. (h) Normalized MDCs at $E = E_F$ for OD30K and OD23K.

strong anisotropy in the spectral response indicates a connection to the anisotropic pseudogap, which manifests itself only in the antinodal region.

Overall, the combination of ARPES and magnetotransport data presents a consistent picture in which the pseudogap regime in overdoped Bi2201 ends at a doping level ($p^* \sim 0.21$) corresponding to $T_c/T_c^{\max} \sim 0.8$. This is significant as it confirms that the p to $1+p$ crossover in the low-T Hall number $n_H(0)$ recently reported in Bi2201 [24,25] is not a consequence of pseudogap closure, but rather reflects a gradual crossover from incoherent to coherent transport as the system is doped across the strange metal regime beyond p^* [24,26]. In Ref. [25], it was claimed, based on complementary NMR measurements, that highly overdoped OD18K and OD10K also reside within the pseudogap regime with correspondingly low T^* values of 40 K and 25 K, respectively. The marked change in $n_H(0)$ for these two samples was then attributed to a recovery of pseudogapped states. It should be noted, however, that the marked change in R_H between the two samples extends to temperatures far higher than T^* [25], indicating a disconnect between the p to $1+p$ crossover and the pseudogap itself. Subsequent high-field specific heat measurements on Bi2201 crystals with T_c values between 10 K and 18 K revealed an enhanced electronic specific heat C_{el}/T upon approaching the putative p^* (corresponding to $T_c \sim 8$ K) [58–66]. It is not yet established, however, whether this enhancement is due to an approach to p^* or to the vHs which is crossed around $p = p_2^{sc}$ [22].

In closing, we remark that if, as the NMR results imply, the pseudogap in Bi2201 does survive out to $T_c/T_c^{\max} \sim 0.25$ ($p_P = 0.255$), then given the identical form of $\rho_{ab}(T)$ in LSCO ($p > p^*$) and Bi2201 ($p_P < p^*$) highlighted in Fig. 2, one would be forced to conclude that the form of $\rho_{ab}(T)$ in overdoped cuprates is not influenced in any way by the presence or absence of the antinodal pseudogap, a conclusion that would bring into question three decades of research. If, on the other hand, the reduction in K_s and $(T_1T)^{-1}$ reported below 60 K for $p_P > 0.21$ was a consequence of fluctuating superconductivity, then the controversies surrounding the phase diagram of Bi2201 may finally be resolved.

IV. SUMMARY

To summarize, from a comparison of the form of $\rho_{ab}(T)$ in overdoped Bi2201 with corresponding curves in overdoped LSCO, an estimate of the doping level in the former has been obtained and the subsequent $T_c(p)$ parabola in Bi2201 is found to follow the same generic form as for other cuprate families. Nevertheless, our accompanying ARPES study indicates that a discrepancy still exists between the ARPES-derived Luttinger count and the Presland-derived p values (summarized in Table I), the origin of which remains unresolved.

Inspection of the $d\rho_{ab}/dT$ curves suggests that resistive signatures of the pseudogap disappear at a doping level $p_P^* \sim 0.21$ that is again comparable to that realized in other cuprates. To distinguish between signatures of pseudogap

formation and superconducting fluctuations beyond p^*, we used high magnetic fields to suppress superconductivity but failed to find any marked signatures of pseudogap formation in $d\rho_{ab}/dT$ for $p_P > 0.21$. This conclusion is further supported by ARPES measurements across p^* that reveal a loss of gaplike features in the normal state and a crossover from incoherent to coherent spectral functions at the antinodes similar to that observed in Bi2212 [17]. It remains to be seen whether the low-T suppression in the density of states inferred from NMR measurements in highly doped Bi2201 can be attributed fully to superconducting fluctuations. If so, it may bring closure to a long-standing controversy in the field and strengthen the notion that the evolution of phases in p-doped cuprates is determined primarily by the number of doped holes in the CuO_2 planes.

ACKNOWLEDGMENTS

We thank J. Ayres, S. Wiedmann, M. Allan, I. Božović, T. Kondo, and T. Takeuchi for insightful discussions and T. Kondo and T. Takeuchi for providing a subset of the Bi2201 crystals. We acknowledge the support of the High Field Magnet Laboratory (HFML) at Radboud University, member of the European Magnetic Field Laboratory (EMFL), also supported by the EPSRC (Ref. No. EP/N01085X/1 and EP/R011141/1), and the former Foundation for Fundamental Research on Matter (FOM), which is financially supported by the Netherlands Organisation for Scientific Research (NWO) (Grant No. 16METL01, "Strange Metals"). Part of this work was also supported by the European Research Council (ERC) under the European Union's Horizon 2020 research and innovation programme (Grant Agreement No. 835279-Catch-22).

[1] B. Keimer, S. A. Kivelson, M. R. Norman, S. Uchida, and J. Zaanen, From quantum matter to high-temperature superconductivity in copper oxides, Nature (London) **518**, 179 (2015).

[2] M. R. Presland, J. L. Tallon, R. G. Buckley, R. S. Liu, and N. E. Flower, General trends in oxygen stoichiometry effects on T_c in Bi and Tl superconductors, Physica C **176**, 95 (1991).

[3] A. R. Moodenbaugh, X. Youwen, M. Suenaga, T. J. Folkerts, and R. N. Shelton, Superconducting properties of $La_{2-x}Ba_xCuO_4$, Phys. Rev. B **38**, 4596 (1988).

[4] A. Yamamoto, W.-Z. Hu, and S. Tajima, Thermoelectric power and resistivity of $HgBa_2CuO_{4+\delta}$ over a wide doping range, Phys. Rev. B **63**, 024504 (2000).

[5] R. Liang, D. A. Bonn, and W. N. Hardy, Evaluation of CuO_2 plane hole doping in $YBa_2Cu_3O_{7-\delta}$ single crystals, Phys. Rev. B **73**, 180505(R) (2006).

[6] I. K. Drozdov, I. Pletikosić, C.-K. Kim, K. Fujita, G. D. Gu, J. C. Séamus Davis, P. D. Johnson, I. Božović, and T. Valla, Phase diagram of $Bi_2Sr_2CaCu_2O_{8+\delta}$ revisited, Nat. Commun. **9**, 5210 (2018).

[7] A. F. Bangura, P. M. C. Rourke, T. M. Benseman, M. Matusiak, J. R. Cooper, N. E. Hussey, and A. Carrington, Fermi surface and electronic homogeneity of the overdoped cuprate superconductor $Tl_2Ba_2CuO_{6+\delta}$ as revealed by quantum oscillations, Phys. Rev. B **82**, 140501(R) (2010).

[8] J. L. Tallon, J. G. Storey, J. R. Cooper, and J. W. Loram, Locating the pseudogap closing point in cuprate superconductors: Absence of entrant or reentrant behavior, Phys. Rev. B **101**, 174512 (2020).

[9] T. Kondo, T. Takeuchi, T. Yokoya, S. Tsuda, S. Shin, and U. Mizutani, Hole-concentration dependence of band structure in $(Bi, Pb)_2(Sr, La)_2CuO_{6+\delta}$ determined by the angle-resolved photoemission spectroscopy, J. Electron Spectrosc. Relat. Phenom. **137-140**, 663 (2004).

[10] Y. Ando, Y. Hanaki, S. Ono, T. Murayama, K. Segawa, N. Miyamoto, and S. Komiya, Carrier concentrations in $Bi_2Sr_{2-z}La_zCuO_{6+\delta}$ single crystals and their relation to the Hall coefficient and thermopower, Phys. Rev. B **61**, R14956 (2000).

[11] T. Kondo, Y. Hamaya, A. D. Palczewski, T. Takeuchi, J. S. Wen, Z. J. Xu, G. D. Gu, J. Schmalian, and A. Kaminski, Disentangling Cooper-pair formation above the transition temperature from the pseudogap state in the cuprates, Nat. Phys. **7**, 21 (2011).

[12] S. Kawasaki, C.-T. Lin, P. L. Kuhns, A. P. Reyes, and G.-q. Zheng, Carrier-Concentration Dependence of the Pseudogap Ground State of Superconducting $Bi_2Sr_{2-x}La_xCuO_{6+\delta}$ Revealed by ^{63,65}Cu -NMR in Very High Magnetic Fields, Phys. Rev. Lett. **105**, 137002 (2010).

[13] Y. Ando, Y. Kurita, S. Komiya, S. Ono, and K. Segawa, Electronic Phase Diagram of High-T_c Cuprates from a Mapping of the In-Plane Resistivity Curvature, Phys. Rev. Lett. **93**, 267001 (2004).

[14] Y. He, Y. Yin, M. Zech, A. Soumyanarayanan, M. N. Yee, T. Williams, M. C. Boyer, K. Chatterjee, W. D. Wise, I. Zeljkovic, T. Kondo, T. Takeuchi, H. Ikuta, P. Mistark, R. S. Markiewicz, A. Bansil, S. Sachdev, E. W. Hudson, and J. E. Hoffman, Fermi surface and pseudogap evolution in a cuprate superconductor, Science **344**, 608 (2014).

[15] G.-q. Zheng, P. L. Kuhns, A. P. Reyes, B. Liang, and C.-T. Lin, Critical Point and the Nature of the Pseudogap of Single-Layered Copper-Oxide $Bi_2Sr_{2-x}La_xCuO_{6+\delta}$ Superconductors, Phys. Rev. Lett. **94**, 047006 (2005).

[16] N. Barišić, M. K. Chan, Y. Li, G. Yu, X. Zhao, M. Dressel, A. Smontara, and M. Greven, Universal sheet resistance and revised phase diagram of the cuprate high-temperature superconductors, Proc. Natl. Acad. Sci. USA **110**, 12235 (2013).

[17] S.-D. Chen, M. Hashimoto, Y. He, D. Song, K.-J. Xu, J.-F. He, T. P Devereaux, H. Eisaki, D.-H. Lu, J. Zaanen, and Z.-X. Shen, Incoherent strange metal sharply bounded by a critical doping in Bi2212, Science **366**, 1099 (2019).

[18] S. D. Obertelli, J. R. Cooper, and J. L. Tallon, Systematics in the thermoelectric power of high-T_c oxides, Phys. Rev. B **46**, 14928 (1992).

[19] N. P. Ong, Geometric interpretation of the weak-field Hall conductivity in two-dimensional metals with arbitrary Fermi surface, Phys. Rev. B **43**, 193 (1991).

[20] A. Narduzzo, G. Albert, M. M. J. French, N. Mangkorntong, M. Nohara, H. Takagi, and N. E. Hussey, Violation of the isotropic mean free path approximation for overdoped $La_{2-x}Sr_xCuO_4$, Phys. Rev. B **77**, 220502(R) (2008).

[21] I. Tsukada and S. Ono, Negative Hall coefficients of heavily overdoped $La_{2-x}Sr_xCuO_4$, Phys. Rev. B **74**, 134508 (2006).

[22] Y. Ding, L. Zhao, H.-T. Yan, Q. Gao, J. Liu, C. Hu, J.-W. Huang, C. Li, Y. Xu, Y.-Q. Cai, H.-T. Rong, D.-S. Wu, C.-Y. Song, H.-X. Zhou, X.-L. Dong, G.-D. Liu, Q.-Y. Wang, S.-J. Zhang, Z.-M. Wang, F.-F. Zhang *et al.*, Disappearance of superconductivity and a concomitant Lifshitz transition in heavily overdoped $Bi_2Sr_2CuO_6$ superconductor revealed by angle-resolved photoemission spectroscopy, Chin. Phys. Lett. **36**, 017402 (2018).

[23] P. M. C. Rourke, I. Mouzopoulou, X. Xu, C. Panagopoulos, Y. Wang, B. Vignolle, C. Proust, E. V. Kurganova, U. Zeitler, Y. Tanabe, T. Adachi, Y. Koike, and N. E. Hussey, A detailed de Haas-van Alphen effect study of the overdoped cuprate $Tl_2Ba_2CuO_{6+\delta}$, New J. Phys. **12**, 105009 (2010).

[24] C. Putzke, S. Benhabib, W. Tabis, J. Ayres, Z. Wang, L. Malone, S. Licciardello, J. Lu, T. Kondo, T. Takeuchi, N. E. Hussey, J. R. Cooper, and A. Carrington, Reduced Hall carrier density in the overdoped strange metal regime of cuprate superconductors, Nat. Phys. **17**, 826 (2021).

[25] M. Lizaire, A. Legros, A. Gourgout, S. Benhabib, S. Badoux, F. Laliberté, M.-E. Boulanger, A. Ataei, G. Grissonnanche, D. LeBoeuf, S. Licciardello, S. Wiedmann, S. Ono, S. Kawasaki, G.-Q. Zheng, N. Doiron-Leyraud, C. Proust, and L. Taillefer, Transport signatures of the pseudogap critical point in the cuprate superconductor $Bi_2Sr_{2-x}La_xCuO_{6+\delta}$, Phys. Rev. B **104**, 014515 (2021).

[26] J. Ayres, M. Berben, M. Čulo, Y.-T. Hsu, E. van Heumen, Y. Huang, J. Zaanen, T. Kondo, T. Takeuchi, J. R. Cooper, C. Putzke, S. Friedemann, A. Carrington, and N. E. Hussey, Incoherent transport across the strange metal regime of highly overdoped cuprates, Nature (London) **595**, 661 (2021).

[27] M. Horio, K. Hauser, Y. Sassa, Z. Mingazheva, D. Sutter, K. Kramer, A. Cook, E. Nocerino, O. K. Forslund, O. Tjernberg, M. Kobayashi, A. Chikina, N. B. M. Schröter, J. A. Krieger, T. Schmitt, V. M. Strocov, S. Pyon, T. Takayama, H. Takagi, O. J. Lipscombe, S. M. Hayden, M. Månsson *et al.*, Three-Dimensional Fermi Surface of Overdoped La-Based Cuprates, Phys. Rev. Lett. **121**, 077004 (2018).

[28] I. M. Vishik. N. Barišić, M. K. Chan, Y. Li, D. D. Xia, G. Yu, X. Zhao, W. S. Lee, W. Meevasana, T. P. Devereaux, M. Greven, and Z. X. Shen, Angle-resolved photoemission spectroscopy study of $HgBa_2CuO_{4+\delta}$, Phys. Rev. B **89**, 195141 (2014).

[29] M. Platé, J. D. F. Mottershead, I. S. Elfimov, D. C. Peets, R. Liang, D. A. Bonn, W. N. Hardy, S. Chiuzbaian, M. Falub, M. Shi, L. Patthey, and A. Damascelli, Fermi Surface and Quasiparticle Excitations of Overdoped $Tl_2Ba_2CuO_{6+\delta}$, Phys. Rev. Lett. **95**, 077001 (2005).

[30] V. B. Zabolotnyy, S. V. Borisenko, A. A. Kordyuk, J. Geck, D. S. Inosov, A. Koitzsch, J. Fink, M. Knupfer, B. Büchner, S.-L. Drechsler, B. Berger, A. Erb, M. Lambacher, L. Patthey, V. Hinkov, and B. Keimer, Momentum and temperature dependence of renormalization effects in the high-temperature superconductor $YBa_2Cu_3O_{7-\delta}$, Phys. Rev. B **76**, 064519 (2007).

[31] J. Chang, M. Månsson, S. Pailhès, T. Claesson, O. J. Lipscombe, S. M. Hayden, L. Patthey, O. Tjernberg, and J. Mesot, Anisotropic breakdown of Fermi-liquid quasiparticle excitations in overdoped $La_{2-x}Sr_xCuO_4$, Nat. Commun. **4**, 1 (2013).

[32] Y. Fang, G. Grissonnanche, A. Legros, S. Verret, F. Laliberte, C. Collignon, A. Ataei, M. Dion, J. Zhou, D. Graf, M. J. Lawler, P. Goddard, L. Taillefer, and B. J. Ramshaw, Fermi surface transformation at the pseudogap critical point of a cuprate superconductor, Nat. Phys. (2022).

[33] M. Hashimoto, T. Yoshida, H. Yagi, M. Takizawa, A. Fujimori, M. Kubota, K. Ono, K. Tanaka, D. H. Lu, Z.-X. Shen, S. Ono, and Y. Ando, Doping evolution of the electronic structure in the single-layer cuprate $Bi_2Sr_{2-x}La_xCuO_{6+\delta}$, Phys. Rev. B **77**, 094516 (2008).

[34] T. Valla, P. Pervan, I. Pletikosić, I. K. Drozdov, A. K. Kundu, A. Wu, and G. D. Gu, Hole-like Fermi surface in the overdoped non-superconducting $Bi_{1.8}Pb_{0.4}Sr_2CuO_{6+\delta}$, Europhys. Lett. **134**, 17002 (2021).

[35] T. Takeuchi, T. Kondo, T. Kitao, H. Kaga, H. Yang, H. Ding, A. Kaminski, and J. C. Campuzano, Two- to Three-Dimensional Crossover in the Electronic Structure of (Bi, Pb)$_2$(Sr, La)$_2CuO_{6+\delta}$ from Angle-Resolved Photoemission Spectroscopy, Phys. Rev. Lett. **95**, 227004 (2005).

[36] See Supplemental Material at http://link.aps.org/supplemental/10.1103/PhysRevMaterials.6.044804 for the full zero-field $\rho_{ab}(T)$ curves of the Bi2201 crystals shown in Fig. 3, a collection of Bi2201 and LSCO Luttinger count data, underlying Fermi surface maps and tight-binding fits, a comparison between near-nodal and anti-nodal ARPES intensity images in overdoped Bi2201 at $T = 150$ K, a discussion of the experimental uncertainty in the determination of $p_{\rm P}$, a detailed discussion of the drop in K_s below $T_{\rm SF}$ in various hole-doped cuprates, a comparison of T^* and $T_{\rm SF}$ in Bi2201 measured by NMR and transport, and an inspection of the H/T scaling in overdoped Bi2201, as well as a detailed discussion of the upward deviations from T-linear resistivity in optimally and overdoped Bi2201.

[37] S. Badoux, W. Tabis, F. Laliberté, G. Grissonnanche, B. Vignolle, D. Vignolles, J. Béard, D. A. Bonn, W. N. Hardy, R. Liang, N. Doiron-Leyraud, L. Taillefer, and C. Proust, Change of carrier density at the pseudogap critical point of a cuprate superconductor, Nature (London) **531**, 210 (2016).

[38] N. E. Hussey, Phenomenology of the normal state in-plane transport properties of high-T_c cuprates, J. Phys.: Condens. Matter **20**, 123201 (2008).

[39] S. H. Naqib, J. R. Cooper, J. L. Tallon, and C. Panagopoulos, T-dependence of electrical resistivity of high-T_c cuprates - from pseudogap to overdoped regions, Physica C **387**, 365 (2003).

[40] R. A. Cooper, Y. Wang, B. Vignolle, O. J. Lipscombe, S. M. Hayden, Y. Tanabe, T. Adachi, Y. Koike, M. Nohara, H. Takagi, C. Proust, and N. E. Hussey, Anomalous criticality in the electrical resistivity of $La_{2-x}Sr_xCuO_4$, Science **323**, 603 (2009).

[41] N. E. Hussey, J. Buhot, and S. Licciardello, A tale of two metals: contrasting criticalities in the pnictides and hole-doped cuprates, Rep. Prog. Phys. **81**, 052501 (2018).

[42] N. E. Hussey, R. A. Cooper, X. Xu, Y. Wang, I. Mouzopoulou, B. Vignolle, and C. Proust, Dichotomy in the T-linear resistivity in hole-doped cuprates, Philos. Trans. R. Soc. A **369**, 1626 (2011).

[43] Given that in LSCO beyond $x = 0.20$, the Fermi surface topology changes from hole- to electronlike, the real carrier density should be $1 - p$. However, there is no clear evidence from any transport property that the carrier density in LSCO suddenly transitions from 1.2 to 0.8 carriers for $x > 0.20$. This suggests that, at least in the doping range of interest, as holes continue to be doped into the CuO_2 plane, the smooth and continuous decrease in the magnitude of resistivity with increasing

x implies that the system is best described as containing $1 + p$ holes, rather than $1 - p$ electrons.

[44] B. Bucher, P. Steiner, J. Karpinski, E. Kaldis, and P. Wachter, Influence of the Spin Gap on the Normal State Transport in $YBa_2Cu_4O_8$, Phys. Rev. Lett. **70**, 2012 (1993).

[45] T. Watanabe, T. Fujii, and A. Matsuda, Anisotropic Resistivities of Precisely Oxygen Controlled Single-Crystal $Bi_2Sr_2CaCu_2O_{8+\delta}$: Systematic Study on "Spin Gap" Effect, Phys. Rev. Lett. **79**, 2113 (1997).

[46] D. N. Basov, R. Liang, B. Dabrowski, D. A. Bonn, W. N. Hardy, and T. Timusk, Pseudogap and Charge Dynamics in CuO_2 Planes in YBCO, Phys. Rev. Lett. **77**, 4090 (1996).

[47] Y. Ando and T. Murayama, Nonuniversal power law of the Hall scattering rate in a single-layer cuprate $Bi_2Sr_{2-x}La_xCuO_{6+\delta}$, Phys. Rev. B **60**, R6991 (1999).

[48] N. E. Hussey, H. Gordon-Moys, J. Kokalj, and R. H. McKenzie, Generic strange-metal behaviour of overdoped cuprates, J. Phys.: Conf. Ser. **449**, 012004 (2013).

[49] H. Alloul, T. Ohno, and P. Mendels, ^{89}Y NMR Evidence for a Fermi-Liquid Behavior in $YBa_2Cu_3O_{6+x}$, Phys. Rev. Lett. **63**, 1700 (1989).

[50] W. W. Warren, R. E. Walstedt, G. F. Brennert, R. J. Cava, R. Tycko, R. F. Bell, and G. Dabbagh, Cu Spin Dynamics and Superconducting Precursor Effects in Planes Above T_c in $YBa_2Cu_3O_{6.7}$, Phys. Rev. Lett. **62**, 1193 (1989).

[51] S. Ohsugi, Y. Kitaoka, and K. Asayama, Temperature dependence of spin susceptibility of $La_{2_x}Sr_xCuO_4$ - Cu Knight shift measurement, Physica C **282-287**, 1373 (1997).

[52] J. M. Harris, Y. F. Yan, P. Matl, N. P. Ong, P. W. Anderson, T. Kimura, and K. Kitazawa, Violation of Kohler's Rule in the Normal-State Magnetoresistance of $YBa_2Cu_3O_{7-\delta}$ and $La_2Sr_xCuO_4$, Phys. Rev. Lett. **75**, 1391 (1995).

[53] P. M. C. Rourke, I. Mouzopoulou, X. Xu, C. Panagopoulos, Y. Wang, B. Vignolle, C. Proust, E. V. Kurganova, U. Zeitler, Y. Tanabe, T. Adachi, Y. Koike, and N. E. Hussey, Phase-fluctuating superconductivity in overdoped $La_{2-x}Sr_xCuO_4$, Nat. Phys. **7**, 455 (2011).

[54] I. M. Hayes, R. D. McDonald, N. P. Breznay, T. Helm, P. J. Moll, M. Wartenbe, A. Shekhter, and J. G. Analytis, Scaling between magnetic field and temperature in the high-temperature superconductor $BaFe_2(As_{1-x}P_x)_2$, Nat. Phys. **12**, 916 (2016).

[55] S. Ono, Y. Ando, T. Murayama, F. F. Balakirev, J. B. Betts, and G. S. Boebinger, Metal-to-Insulator Crossover in the Low-Temperature Normal State of$Bi_2Sr_{2-x}La_xCuO_{6+\delta}$, Phys. Rev. Lett. **85**, 638 (2000).

[56] C. E. Matt, C. G. Fatuzzo, Y. Sassa, M. Mansson, S. Fatale, V. Bitetta, X. Shi, S. Pailhes, M. H. Berntsen, T. Kurosawa, M. Oda, N. Momono, O. J. Lipscombe, S. M. Hayden, J. Q. Yan, J.-S. Zhou, J. B. Goodenough, S. Pyon, T. Takayama, H. Takagi, O. Tjernberg *et al.*, Electron scattering, charge order, and pseudogap physics in $La_{1.6-x}Nd_{0.4}Sr_xCuO_4$: An angle-resolved photoemission spectroscopy study, Phys. Rev. B **92**, 134524 (2015).

[57] C. Collignon, S. Badoux, S. A. A. Afshar, B. Michon, F. Laliberté, O. Cyr-Choinière, J.-S. Zhou, S. Licciardello, S. Wiedmann, N. Doiron-Leyraud, and L. Taillefer, Fermi-surface transformation across the pseudogap critical point of the cuprate superconductor $La_{1.6-x}Nd_{0.4}Sr_xCuO_4$, Phys. Rev. B **95**, 224517 (2017).

[58] C. Girod, D. LeBoeuf, A. Demuer, G. Seyfarth, S. Imajo, K. Kindo, Y. Kohama, M. Lizaire, A. Legros, A. Gourgout, H. Takagi, T. Kurosawa, M. Oda, N. Momono, J. Chang, S. Ono, G.-q. Zheng, C. Marcenat, L. Taillefer, and T. Klein, Normal state specific heat in the cuprate superconductors $La_{2-x}Sr_xCuO_4$ and $Bi_2Sr_{2-x}La_xCuO_{6+\delta}$ near the critical point of the pseudogap phase, Phys. Rev. B **103**, 214506 (2021).

[59] H. Takagi, T. Ido, S. Ishibashi, M. Uota, S. Uchida, and Y. Tokura, Superconductor-to-nonsuperconductor transition in $(La_{1-x}Sr_x)_2CuO_4$ as investigated by transport and magnetic measurements, Phys. Rev. B **40**, 2254 (1989).

[60] Y. Wang, J. Yan, L. Shan, H.-H. Wen, Y. Tanabe, T. Adachi, and Y. Koike, Weak-coupling d-wave BCS superconductivity and unpaired electrons in overdoped $La_{2-x}Sr_xCuO_4$ single crystals, Phys. Rev. B **76**, 064512 (2007).

[61] S. Licciardello, N. Maksimovic, J. Ayres, J. Buhot, M. Čulo, B. Bryant, S. Kasahara, Y. Matsuda, T. Shibauchi, V. Nagarajan, J. G. Analytis, and N. E. Hussey, Coexistence of orbital and quantum critical magnetoresistance in $FeSe_{1-x}S_x$, Phys. Rev. Research **1**, 023011 (2019).

[62] P. Giraldo-Gallo, J. A. Galvis, Z. Stegen, K. A. Modic, F. F. Balakirev, J. B. Betts, X. Lian, C. Moir, S. C. Riggs, J. Wu, A. T. Bollinger, X. He, I. Božović, B. J. Ramshaw, R. D. McDonald, G. S. Boebinger, and A. Shekhter, Scale-invariant magnetoresistance in a cuprate superconductor, Science **361**, 479 (2018).

[63] R. Daou, N. Doiron-Leyraud, D. LeBoeuf, S. Y. Li, F. Laliberté, O. Cyr-Choinière, Y. J. Jo, L. Balicas, J.-Q. Yan, J.-S. Zhou, J. B. Goodenough, and L. Taillefer, Linear temperature dependence of resistivity and change in the Fermi surface at the pseudogap critical point of a high-T_c superconductor, Nat. Phys. **5**, 31 (2009).

[64] M. Berben, J. Ayres, C. Duffy, R. D. H. Hinlopen, Y.-T. Hsu, M. Leroux, I. Gilmutdinov, M. Massoudzadegan, D. Vignolles, Y. Huang, T. Kondo, T. Takeuchi, J. R. Cooper, S. Friedemann, A. Carrington, C. Proust, and N. E. Hussey, Compartmentalizing the cuprate strange metal, arXiv:2203.04867.

[65] T. Nakano, N. Momono, C. Manabe, Y. Miura, M. Oda, and M. Ido, Magnetic susceptibility of superconducting $La_{2_x}Sr_xCuO_4$, Czech. J. Phys. **46**, 1153 (1996).

[66] C. Panagopoulos, T. Xiang, W. Anukool, J. R. Cooper, Y. S. Wang, and C. W. Chu, Superfluid response in monolayer high-T_c cuprates, Phys. Rev. B **67**, 220502(R) (2003).